Electrochemical investigations of the interaction of metal chelates with DNA. 3. Electrogenerated chemiluminescent investigation of the interaction of tris(1,10-phenanthroline)ruthenium(II) with DNA

Michael T. Carter, and Allen J. Bard

More About This Article

The permalink http://dx.doi.org/10.1021/bc00004a005 provides access to:

- Links to articles and content related to this article
- Copyright permission to reproduce figures and/or text from this article

Electrochemical Investigations of the Interaction of Metal Chelates with DNA. 3. Electrogenerated Chemiluminescent Investigation of the Interaction of Tris(1,10-phenanthroline)ruthenium(II) with DNA

Michael T. Carter[†] and Allen J. Bard[*]

Department of Chemistry, The University of Texas at Austin, Austin, Texas 78712. Received March 28, 1990

The electrogenerated chemiluminescence (ECL) that results from the oxidation of tris(1,10-phenanthroline)ruthenium(II), at a gold electrode in the presence of oxalate, was used to investigate the interaction of the Ru(II) chelate with calf thymus DNA. The decrease in ECL emission from the excited state, $Ru(phen)_3^{2+*}$, in the presence of DNA, is ascribed to binding of the chelate to the DNA strand. An ECL titration of the metal complex with DNA allowed determination of the equilibrium constant (K) and binding-site size (s) for association of $Ru(phen)_3^{2+}$, under the assumption that only the free metal complex contributes to the observed emission. In 25 mM $Na_2C_2O_4$, 2 mM phosphate buffer, pH 5, 0.05% Tween-20, 0.05% Triton X-100, regression based on the McGhee/von Hippel model, which accounts for free base pair gaps between binding sites, yielded K = 8.1 ($\pm$ 0.2) × 10^3 M^{-1} and s = 4 bp.

INTRODUCTION

We describe the application of electrogenerated chemiluminescence (ECL) measurements to an investigation of the binding of tris(1,10-phenanthroline)ruthenium(II), $Ru(phen)_3^{2+}$, to calf thymus DNA. ECL has been used to investigate electrode reactions that lead to excited states, with applications to analytical problems (1). Many studies have been carried out on ECL systems based on chelates of Ru(II), e.g. $Ru(bpy)_3^{2+}$ (bpy = 2,2'-bipyridine), $Ru(phen)_3^{2+}$, and their derivatives, which yield emissions characteristic of the RuL_3^{2+*} excited state via direct annihilation of the 1+ and 3+ oxidation states in cyclic potential step experiments (2–6), or via generation of the excited state in a single potential step, in the presence of a reactant such as oxalate or peroxydisulfate that generates a strong oxidant or reductant intermediate (e.g., $CO_2^{\bullet-}$ or $SO_4^{\bullet-}$) (7–10). Analytical methods, e.g., for oxalate or with Ru chelate tags (10), based on ECL have been reported. An ECL analysis is carried out in an electrochemical cell containing appropriate reagents (e.g., the Ru species, oxalate, buffer). The imposition of the appropriate electrical signal to the working electrode causes light emission. The fact that no excitation light is employed in ECL, as it is in photoluminescence, leads to high sensitivities in ECL detection. Moreover, the specific nature of the ECL reaction, with control over both electrochemical and spectroscopic variables, promotes high selectivity.

Barton has reported (11–13) the use of enantiomers of $Ru(phen)_2^{2+}$ (14), $Ru(phen)_3^{2+}$, $Ru(DIP)_3^{2+}$ (DIP = 4,7-diphenyl-1,10-phenanthroline) (15–19), and $Ru(TMP)_3^{2+}$ (TMP = 3,4,7,8-tetramethyl-1,10-phenanthroline) (20) as chiral probes for the B, Z, and A conformations of DNA. Metal-activated cleavage of DNA strands can also be accomplished by Ru(II) chelates (21, 22). Because of the wide interest in $Ru(phen)_3^{2+}$ and related complexes in the study of DNA conformation and cleavage and of chemiluminescent systems to biological problems (23–25), we have chosen to investigate the ECL of $Ru(phen)_3^{2+}$ in the presence of DNA, as a means of characterizing the binding of the luminescor to the DNA strand.

To our knowledge, ECL studies of equilibria for binding of metal chelates to DNA have not been reported previously. ECL provides a useful extension of our previously reported voltammetric studies of the binding of metal chelates to DNA (26, 27). Detection of luminescence can be achieved with high precision and has the advantage compared to voltammetric and spectrophotometric measurements that very low concentrations of complex (e.g., micromolar to nanomolar) can be used. As shown below, analysis of the binding data from titration experiments is simplified, in the case of the $Ru(phen)_3^{2+}$–oxalate ECL system, where the oxalate species does not interact with DNA.

EXPERIMENTAL PROCEDURES

Materials. Calf thymus DNA was purchased from Sigma Chemical Co. (St. Louis, MO) and used as received. Previous studies with this material (26, 27) have shown no differences in binding studies with as-received and purified material. The details of the handling of the DNA have been described previously (26, 27). Tris(1,10-phenanthroline)ruthenium(II) dichloride, $Ru(phen)_3Cl_2$, was purchased from Aldrich Chemical Co. (Milwaukee, WI). The as-received material was dissolved in hot water to filter out an unidentified, insoluble, black substance. The filtrate was concentrated to a small volume and allowed to evaporate to dryness at room temperature to obtain the metal complex. Tween-20 was obtained from Sargent-Welch (Irving, TX) and Triton X-100 was from Fluka Chemical Corp. (Ronkonkoma, NY). Tripropylamine (TPrA) (98%) was obtained from Aldrich and used as received. All other chemicals for preparation of electrolytes were reagent grade and used without further purification. Solutions were prepared with high-purity water from a Millipore Milli-Q reagent water system.

Procedures. Experiments were carried out with solutions of $Ru(phen)_3^{2+}$ with either oxalate or TPrA buffered to the pH for optimum ECL response. Concentrations of DNA were measured in electrolyte 1 [25

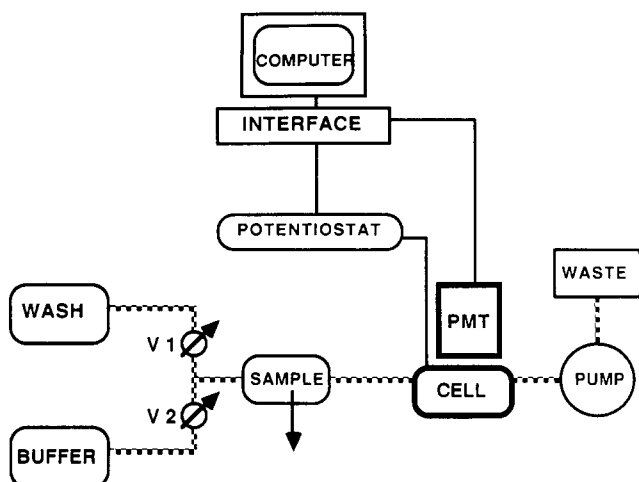**Figure 1.** Block diagram of an Origen Analyzer.

mM $Na_2C_2O_4$, 2 mM H_3PO_4, 0.05% (w/v) Tween-20, 0.05% w/v) Triton X-100, adjusted to pH 5 with NaOH] and electrolyte 2 (25 mM TPrA, 7.2 mM H_2SO_4, 16.1 mM Na_2SO_4, 0.05% Tween-20, 0.05% Triton X-100, adjusted to pH 5 with NaOH) assuming ϵ_{260} = 6600 M^{-1} cm^{-1} (*28*). Concentrations of $Ru(phen)_3^{2+}$ in electrolytes 1 and 2 were measured by assuming ϵ_{447} = 19 000 M^{-1} cm^{-1} (*29*). Solutions of DNA and $Ru(phen)_3^{2+}$ in electrolytes 1 and 2 showed the same absorbances at λ_{max} as in equimolar solutions in 50 mM NaCl. The surfactants Tween-20 and Triton X-100 were added to prevent bubble formation in the flow ECL cell in the analyzer and to promote more effective cleaning of the cell in the flushes with pure electrolyte between samples (*32*). In a recent ECL study of the interaction of another metal chelate with DNA, to be reported elsewhere, we have found procedures where addition of surfactant can be avoided.

For ECL measurements, 0.6 mL of the solution of interest (8–9 μM $Ru(phen)_3^{2+}$ containing different excesses of nucleotides) was pumped through the flow cell of the ECL analyzer described below, in a flow stream of the appropriate electrolyte. Measurements were taken during a potential sweep, under quiescent solution conditions. The potential applied to the potentiostat was scanned linearly from 0.565 to 2.4 V vs Ag/AgCl, at 438 mV/s. The ECL cell configuration used in the analyzer resulted in a significant uncompensated resistance between working and reference electrodes, so the actual working electrode potential was less positive, but clearly encompassed the Ru(II) oxidation wave. Luminescence from the Ru-$(phen)_3^{2+*}$ excited state was measured in 34-ms intervals, during a scan. All measurements were obtained on air-equilibrated samples, at the ambient temperature of the laboratory (23–25 °C). Five replicate measurements were performed on each sample.

Stock solutions of DNA (2–3 mM nucleotide phosphate, NP) and $Ru(phen)_3^{2+}$ (1 mM) were prepared fresh for each series of experiments and discarded immediately after use. All glassware was silanized with a 5% solution of trimethylchlorosilane in toluene.

Instrumentation. Electrogenerated chemiluminescence (ECL) was measured on an Origen 1 Analyzer (IGEN, Inc., Rockville, MD), an automated, computer-controlled (IBM PS/2 Model 25) flow system for ECL analysis of different types of samples (Figure 1). In this system the sample is introduced into a flow stream of the appropriate solution and is pumped into an electrochemical flow cell, equipped with a Plexiglas window where the working electrode surface is viewed by a photomultiplier tube
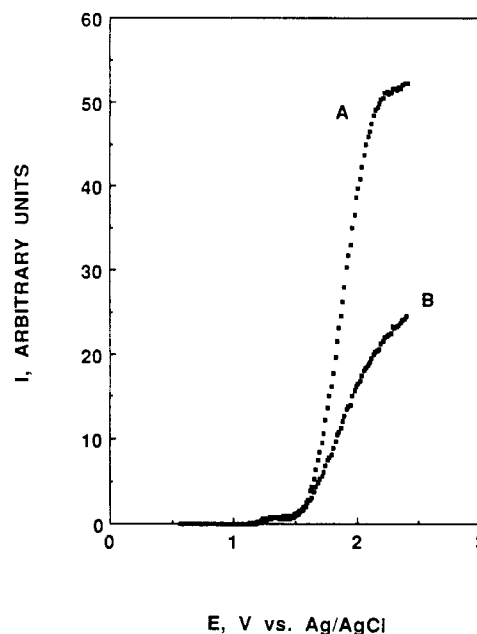

E, V vs. Ag/AgCl

Figure 2. Typical intensity–potential curves for 9.2 μM Ru-$(phen)_3^{2+}$ (A) in the absence and (B) in the presence of 0.28 mM nucleotide phosphate.

(PMT). The working and counter electrodes were gold disks (geometric area = 0.071 cm^2) and the reference electrode was Ag/AgCl (3 M NaCl) located downstream of the flow cell. Cell resistances were 2600 Ω (working-to-counter electrode) and 7.2 × 10^4 Ω (working-to-reference-electrode leads), in electrolyte 1, as measured with a Yellow Springs Instruments Model 35 conductance meter. The thickness of the solution layer in the cell was ca. 0.5 mm. During analysis, the flow was stopped and a programmed potential sweep was applied to the working electrode. ECL during the sweep was detected with a Hamamatsu R 1104 PMT, operated at 850 V.

Spectroscopic measurements were done on a Hewlett-Packard Model 8450A dual-beam spectrophotometer. Cyclic voltammetry (CV) and square wave voltammetry (SWV) were performed on a Bioanalytical Systems (BAS) Model 100 electrochemical analyzer. SWV was performed with square wave amplitude = 25 mV and step height = 5 mV. The square wave frequency was 15 Hz. Working electrodes for voltammetry were either a BAS glassy carbon disk (geometric area = 0.071 cm^2) or a gold disk sealed in glass (geometric area = 0.03 cm^2). A Pt flag served as the counter electrode and the reference was a saturated calomel electrode (SCE). Analysis of titration data from ECL experiments was performed using nonlinear-regression routines available from the SAS statistical software package (The SAS Institute, Cary, NC) on an IBM 3081D computer.

RESULTS

Effect of DNA on ECL Emission. A typical intensity (*I*)–potential curve for the $Ru(phen)_3^{2+}$–oxalate system (electrolyte 1) is shown in Figure 2, for a total concentration (C_t) of $Ru(phen)_3^{2+}$ of 9.2 μM. The potentials shown in Figure 2 should be considered as values applied to the potentiostat because of the large, uncompensated resistance of the electrochemical cell. Onset of ECL from Ru-$(phen)_3^{2+*}$ occurred at ca. 1.25 V vs Ag/AgCl and reached a maximum at ca. 2.0 V, in the absence of DNA. In the presence of 0.28 mM nucleotide phosphate [NP] (Figure 2B, i.e., at a ratio of nucleotide phosphate, NP, to metal complex, R, of 30), the intensity decreased to 48% of that in the absence of DNA. Since the solution layer through
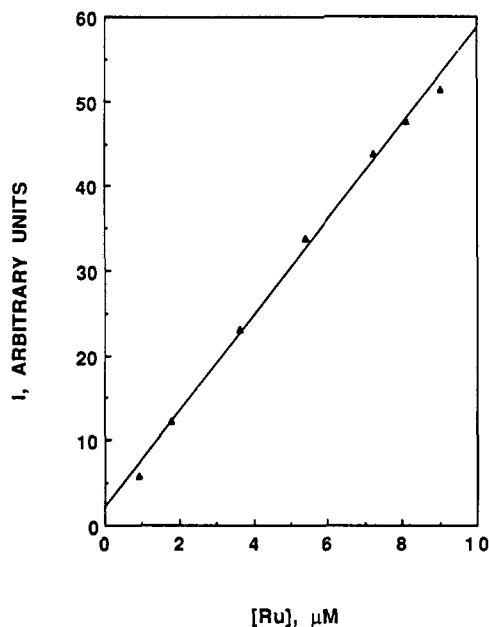
Figure 3. Detector response for concentrations of Ru(phen)$_3^{2+}$ varied between 9.02 and 0.9 μM, in DNA-free solution.

which the emitted light passes is thin (ca. 0.5 mm), the decrease in ECL in the presence of DNA cannot be attributed to scattering by DNA. Additionally, at higher photomultiplier voltages, where background emission from electrolyte could be measured, the presence of a large concentration of DNA caused no decrease in the background. For example, at [NP] = 0, the emission intensity, I, was 33 (arbitrary units), and at [NP] = 1.4 mM, I = 55. Thus, in the presence of DNA, background emission actually increased slightly. Significant adsorption of DNA onto the gold electrode during a measurement would be expected to have the opposite effect, especially if light scattering occurred. Irreversible adsorption of DNA would also be expected to yield decreases in intensity upon repetitive runs on the same Ru(II)/DNA mixture. However, all measurements during a series of experiments were reproducible, regardless of the order in which the solutions were sampled.

A plot of the peak ECL emission intensity, I, against concentration of Ru(II), in the absence of DNA, was linear, as shown in Figure 3. Here, the concentrations of Ru(II) were chosen to span the range of observed decreases in ECL intensity, as a function of DNA concentration, in titration experiments (see below). Linearity of the response to Ru(II) concentration is important in this system, since it bears directly upon the model used to fit titration data. The small intercept represents background emission in the oxalate, as previously observed at other electrode materials in studies of Ru(bpy)$_3^{2+}$ system ECL (10). It has been ascribed to effects of traces of undefined impurity or to inverse photoemission from the metal electrode.

Cyclic Voltammetry in Oxalate Electrolyte. Cyclic voltammograms of electrolyte 1 showed an oxidation wave at 0.7 V vs SCE on the first positive-going scan at a gold disk. Upon subsequent scans, the wave disappeared. The oxidation wave observed on the initial scan corresponds to oxidation of the gold electrode surface. On the second and subsequent scans this wave is absent because the oxide is not reduced by the oxalate in the solution. The oxidation wave only reappeared upon scanning the potential of the electrode from 0.0 to -1.0 V, but subsequent positive-going scans again showed a diminished oxidation wave upon repeated scanning. Direct oxidation of oxalate on
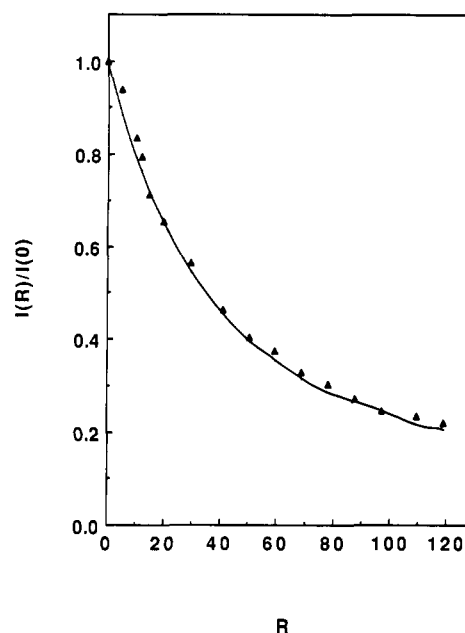

Figure 4. ECL titration of 8.7 μM Ru(phen)$_3^{2+}$ with DNA, in electrolyte 1. Normalized emission intensity vs R, where R = [nucleotide phosphate]/[total Ru] = [NP]/C_t. Points are experimental data and the solid curve represents that calculated based on the equilibrium model of McGhee and von Hippel.

the oxidized gold electrode does not occur until oxidation of Ru(phen)$_3^{2+}$ takes place at $+1.1$ V vs SCE.

Experimental Titration Results. Results of a titration of 8.7 μM Ru(phen)$_3^{2+}$ with DNA, in electrolyte 1, are shown in Figure 4. Experimental data are plotted as peak emission intensity, I, normalized to I at R = 0, [I-(0)] vs R where

$$R = [\text{nucleotide phosphate}]/[\text{total Ru}] = [\text{NP}]/C_t$$

The data were regressed onto eq 3, below, with K determined from a one-parameter fit, for integer values of s (15, 27). The best fit for the experimental curve was K = 8.1 ($\pm$0.2) $\times$ 10^3 M^{-1} and s = 4 bp (solid curve of Figure 4). Extensive sonication of a solution containing 9.0 μM Ru(phen)$_3^{2+}$ and 0.86 mM NP (electrolyte 1) resulted in only ca. 14% increase in ECL intensity after 65 min of treatment. ECL of a solution containing only Ru(phen)$_3^{2+}$ was not affected when sonicated for the same amount of time.

Experiments were performed in which 25 mM tri-n-propylamine (TPrA) was cooxidized with Ru(phen)$_3^{2+}$ to produce ECL (electrolyte 2) (32, 33). The ionic strength and pH of this system was the same as those for electrolyte 1. Since binding of Ru(phen)$_3^{2+}$ to DNA is dependent on ionic strength (18), no difference in normalized ECL intensity would be expected, at the same C_t and R, between the Ru(phen)$_3^{2+}$-oxalate and Ru(phen)$_3^{2+}$-TPrA systems, assuming equal interactions of TPrA and oxalate with DNA. However, $I(R)/I(0)$ was larger, at all R investigated, in the TPrA system than for the corresponding experiment in the oxalate system. For example, at R = 40 (8.8 μM Ru(II)), $I(R)/I(0)$ = 0.47 for oxalate vs 0.63 for TPrA, and at R = 80, $I(R)/I(0)$ = 0.30 for oxalate vs 0.49 for TPrA. As shown in Figure 2, the detector response to ECL in the Ru(phen)$_3^{2+}$-TPrA system was linear with concentration of Ru(II), over a concentration range bracketing the observed decrease in intensity with addition of DNA.

An Equilibrium Binding Model. The peak intensity, I, is a linear function of Ru(phen)$_3^{2+}$ concentration, in the absence of DNA

$$I/I_0 = C/C_0 \qquad (1)$$

where I and I_0 are the peak intensities at concentrations of Ru(II) C and C_0, respectively. A treatment of binding data, based on a modification of the classical Scatchard binding isotherm (34), has been reported by McGhee and von Hippel. This model (35) accounts for the presence of free gaps on DNA which are less than s bp long and thus cannot participate in binding of the metal complex (i.e., the DNA strand cannot be saturated with metal complex). The relevant equation for noncooperative binding, based on an analogous one of Barton et al. (15), with $\nu = C_b/[NP]$, is

$$\frac{\nu}{C_f} = \frac{K}{2}(1 - 2s\nu)\left[\frac{1 - 2s\nu}{1 - 2(s-1)\nu}\right]^{s-1} \qquad (2)$$

where C_b and C_f are the equilibrium concentrations of DNA-bound and free metal complex, respectively, K is the microscopic binding constant, and s is the binding-site size, in base pairs, bp. This may be rewritten to give the normalized ECL intensity as a function of C_t and R:

$$\frac{I(R)}{I(0)} = \left\{\frac{RC_t K}{2}[1 - 2s(X_b/R)] \times \right.$$
$$\left.\left[\frac{1 - 2s(X_b/R)}{1 - 2(s-1)(X_b/R)}\right]^{s-1} + 1\right\}^{-1} \qquad (3)$$

where $I(R)$ and $I(0)$ are the intensities measured at R and $R = 0$, respectively, $C_t = C_b + C_f$, and $X_b = C_b/C_t$, under the assumption that only the free metal complex contributes to ECL. The value of s for the titration data of Figure 4 is in excellent agreement with that determined by Barton (15). K is ca. 30% larger than in the previous determination ($K = 6.3 \times 10^3$ M^{-1}, in 50 mM NaCl, 5 mM Tris, pH 7.1) (15).

Comparison to the Voltammetric Binding Model. We have previously shown that the concentration of bound metal, C_b, as a function of total metal concentration, C_t, binding constant, K, and binding-site size, s, is (26, 27)

$$C_b = \{b - [b^2 - (2K^2C_t[NP]/s)]^{1/2}\}/2K \qquad (4a)$$

$$b = 1 + KC_t + K[NP]/2s \qquad (4b)$$

Equation 4 assumes (1) nonspecific, (2) noncooperative binding, and (3) existence of a single, discreet binding site. Assumption 3 may be interpreted as the ability to saturate the DNA strand with metal complex (i.e., all base pairs can participate in binding). With this model the ECL intensity is given by

$$I(R) = A_f C_f + A_b C_b \qquad (5)$$

where A_f and A_b are constants of proportionality for ECL arising from free and bound metal complex, respectively. This may be rewritten as

$$I(R) = A_f C_f + X A_f C_b \qquad (6a)$$

$$I(0) = A_f C_t \qquad (6b)$$

where X $(0 \leq X \leq 1)$ represents the fraction of total ECL due to bound metal. Combining eqs 6a and 6b gives

$$I(R)/I(0) = r(1 - X) + X \qquad (7a)$$

$$r = C_f/C_t \qquad (7b)$$

Equation 7 reduces to the equivalent of eq 1 when $X = 0$ (i.e., bound metal does not contribute to ECL emission). Note that this assumption allows calculation of binding constant and binding-site size without knowledge of the diffusion coefficients of the free and DNA-bound metal
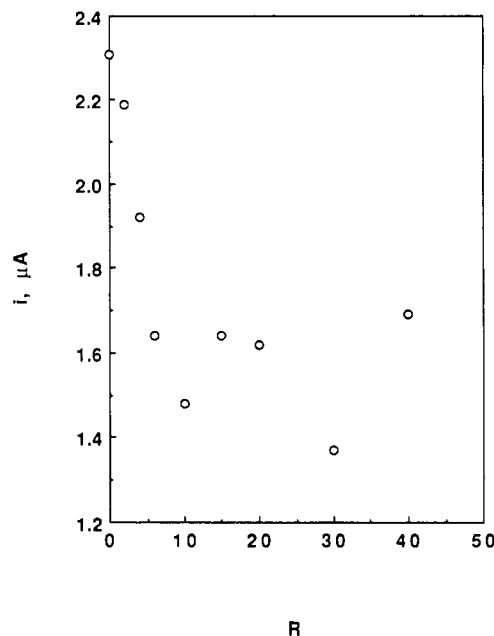

R

Figure 5. Square wave voltammetric titration of 9.2×10^{-5} M Ru(phen)$_6{}^{2+}$ with DNA. The electrolyte was 25 mM Na$_2$C$_2$O$_4$, 2 mM H$_3$PO$_4$, pH 5.0.

complex (D_f and D_b) or of the ECL efficiency for the Ru-(phen)$_3{}^{2+}$–oxalate system. The magnitudes of the binding parameters were calculated via eq 7, again fitting K for integer values of s (26, 27). A plot of the experimental data, superimposed on the best-fit curve, was essentially identical to that shown in Figure 4, except as noted below. The best fit of the experimental data to the simple binding model given above was $K = 9.0$ (± 0.4) $\times 10^4$ M^{-1} and $s = 10$ bp (when $X = 0$), suggesting that some segments of the DNA strand are unavailable for binding. The binding-site size here is much larger than that determined previously for binding of racemic Ru(phen)$_3{}^{2+}$ (in 50 mM NaCl, 5 mM Tris, pH 7.1) to calf thymus DNA (15). While the agreement between experiment and calculations from the two models is about the same for $R \leq 60$, there is slightly better agreement at $R > 60$ when eq 3 is used, vs eq 7. The implications of the titration results are discussed below.

To test further the validity of the assumption that bound metal does not contribute significantly to ECL, additional two-parameter fits were performed in which K and X were determined for $s = 10$ bp. These calculations gave $K = 9.6$ (± 0.8) $\times 10^4$ M^{-1} and $X = 0.02$. The sum of squares deviation obtained here agreed with that from the one-parameter fit of K, above, to within 3%. Thus, we can estimate that at least 98% of the ECL is due to free metal complex and that the assumptions used in fitting titration data are valid, within the error of the measurement.
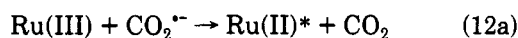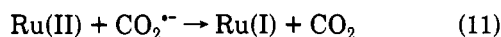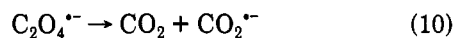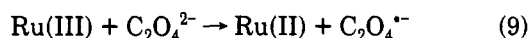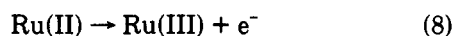
Square Wave Voltammetry. To test the possibility that the surfactants present in the electrolyte used for ECL measurements may interfere with binding of Ru-(phen)$_3{}^{2+}$ to DNA, independent measurements of binding were performed by using square wave voltammetry (SWV). SWV was employed, rather than the cyclic voltammetry or differential pulse voltammetry used in earlier electrochemical experiments (26, 27), because very small concentrations of Ru(II) were used to keep the concentration range equivalent to that in the ECL experiments. Measurements cannot be carried out conveniently with electrolytes without added surfactants in the ECL apparatus described above. Typical results are shown in Figure 5, where the peak current in SWV for oxidation of Ru(phen)$_3{}^{2+}$ to the 3+ ion is plotted

as a function of R. The electrolyte here was electrolyte 1, but without added Triton X-100 or Tween-20. Although SWV measurements at these concentrations are not very precise and the data show appreciable scatter, particularly at larger values of R where the concentration of unbound $Ru(phen)_3^{2+}$ is small, the titration curve in Figure 5 indicates that the binding-site size (s), in the absence of surfactants, is smaller than that found in ECL measurements. A value of s = 10 bp would correspond to R = 20 in Figure 5. The data indicate a value of s closer to 5 bp.
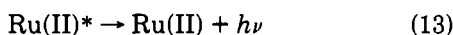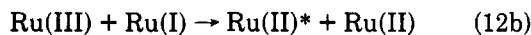
The peak potential of the $Ru(phen)_3^{2+/3+}$ redox couple is severely overlapped by the background oxidation of the electrolyte. Although the data shown in Figure 5 represent background-subtracted peak currents, the background current in the region of Ru(II) oxidation is not particularly reproducible. The result is the scatter in the data shown. Thus, while this experiment suggests that the absence of surfactant causes the apparent value of s to decrease, we could not obtain quantitative results from nonlinear-regression analysis, based on a SWV analogue of our previously reported voltammetric titration method (26, 27). Voltammetric measurements under the electrolyte conditions of the ECL measurements, i.e., with added Triton X-100 or Tween-20, could not be carried out because electroactive components in the surfactant stock solutions interfered with the Ru(II) oxidation wave.

DISCUSSION
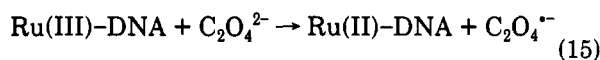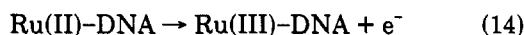
ECL in electrolyte 1 originates from oxidation of $Ru(phen)_3^{2+}$, in the presence of oxalate, according to the following sequence of reactions (8, 10):

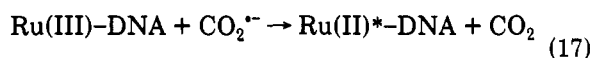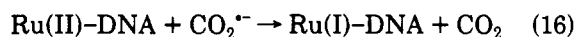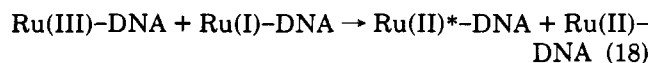$$Ru(II) \rightarrow Ru(III) + e^- \tag{8}$$

$$Ru(III) + C_2O_4^{2-} \rightarrow Ru(II) + C_2O_4^{\cdot-} \tag{9}$$

$$C_2O_4^{\cdot-} \rightarrow CO_2 + CO_2^{\cdot-} \tag{10}$$

$$Ru(II) + CO_2^{\cdot-} \rightarrow Ru(I) + CO_2 \tag{11}$$

$$Ru(III) + CO_2^{\cdot-} \rightarrow Ru(II)^* + CO_2 \tag{12a}$$

or

$$Ru(III) + Ru(I) \rightarrow Ru(II)^* + Ru(II) \tag{12b}$$

$$Ru(II)^* \rightarrow Ru(II) + h\nu \tag{13}$$

where Ru(II) and Ru(III) represent $Ru(phen)_3^{2+}$ and $Ru(phen)_3^{3+}$. In the presence of DNA, the corresponding reaction sequence is

$$Ru(II)-DNA \rightarrow Ru(III)-DNA + e^- \tag{14}$$

$$Ru(III)-DNA + C_2O_4^{2-} \rightarrow Ru(II)-DNA + C_2O_4^{\cdot-} \tag{15}$$

followed by eq 10 and

$$Ru(II)-DNA + CO_2^{\cdot-} \rightarrow Ru(I)-DNA + CO_2 \tag{16}$$

$$Ru(III)-DNA + CO_2^{\cdot-} \rightarrow Ru(II)^*-DNA + CO_2 \tag{17}$$

or

$$Ru(III)-DNA + Ru(I)-DNA \rightarrow Ru(II)^*-DNA + Ru(II)-DNA \tag{18}$$
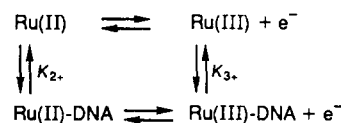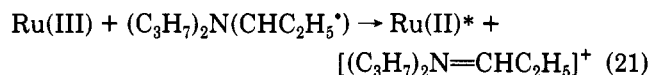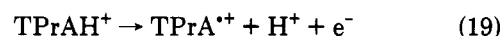
followed by eq 13, where –DNA denotes a metal complex bound to DNA. However the results indicate that emission does not result from Ru(II) bound to DNA. This might be caused by inaccessibility of DNA-bound Ru species to CO_2^- or $C_2O_4^{2-}$ (e.g. because of steric constraints or electrostatic effects due to the negative charge on the DNA

double helix, as discussed below). This reduces this series of reactions to eqs 8–14. The ECL intensity is controlled by the equilibrium binding of the metal chelate to DNA. Combining eqs 8 and 14, by analogy with our previous work (26, 27) and electrochemical studies of the interaction of electroactive species with micelles (36, 37), gives Scheme I.

Scheme I

$$
\begin{array}{ccc}
Ru(II) & \rightleftharpoons & Ru(III) + e^- \\
\updownarrow K_{2^+} & & \updownarrow K_{3^+} \\
Ru(II)-DNA & \rightleftharpoons & Ru(III)-DNA + e^-
\end{array}
$$

The mechanism of light emission in the $Ru(phen)_3^{2+}$–TPrA system has not been elucidated but probably proceeds through a reaction sequence similar to that of $Ru(phen)_3^{2+}$–oxalate, with cooxidation of $Ru(phen)_3^{2+}$ and $TPrAH^+$ producing the excited state-chelate by eq 8, followed by (32, 33, 38)

$$TPrAH^+ \rightarrow TPrA^{\cdot+} + H^+ + e^- \tag{19}$$

$$TPrA^{\cdot+} \rightarrow (C_3H_7)_2N(CHC_2H_5^{\cdot}) + H^+ \tag{20}$$

$$Ru(III) + (C_3H_7)_2N(CHC_2H_5^{\cdot}) \rightarrow Ru(II)^* + [(C_3H_7)_2N=CHC_2H_5]^+ \tag{21}$$

Binding of cations to DNA is driven by release of counterions from the helix (e.g., Na^+) (39, 40). In view of the experimental results described above for the differences in behavior of the oxalate and TPrA systems, it is reasonable that the ECL is essentially due to free $Ru(phen)_3^{2+}$. Since TPrA is fully protonated at pH 5.0 (pK_a = 10.6), these results suggest that bound $Ru(phen)_3^{2+}$ can participate to a small extent in ECL in electrolyte 2, because $TPrAH^+$ can approach the anionic sugar-phosphate backbone of DNA. In electrolyte 1, however, oxalate exists as 84% dianionic and 16% monoanionic forms. Oxalate would not be expected to interact with DNA as strongly as $TPrAH^+$, because of coulombic repulsion. While the reactant $TPrA^{\cdot}$ in eqs 20 and 21 is uncharged, TPrA is initially delivered to the bound Ru species as the protonated form. The results support the assumption that the ECL component from bound metal in the oxalate system can be neglected and are consistent with our previous observations on the lack of influence of DNA on the diffusion of anions, such as $Mo(CN)_8^{4-}$ and $Fe(CN)_6^{3-}$ (26, 27) as well as observations on luminescence quenching of $Ru(phen)_3^{2+}$, bound to DNA, by ferrocyanide (17). The photoluminescence of $Ru(phen)_3^{2+}$ is enhanced upon binding to DNA (15, 17, 18, 41), in the absence of added quencher. The excited state of another intercalator, ethidium, bound to DNA is effectively quenched by cationic species, e.g. methylviologen (42, 43), whereas $Ru(phen)_3^{2+}$ bound to DNA is protected from quenching by anionic species such as $Fe(CN)_6^{4-}$ (17). The enhanced luminescence of $Ru(phen)_3^{2+}$ intercalated into DNA was attributed to "greater rigidity and lower collisional frequency of the molecule when stacked within the helix". This same decreased collisional frequency, with $C_2O_4^{2-}$, $HC_2O_4^-$ and $CO_2^{\cdot-}$, would decrease excited-state formation. The lower diffusion coefficient of $Ru(phen)_3^{2+}$ when bound to DNA would also decrease the contribution from bound $Ru(phen)_3^{2+}$. The small increase in ECL, in experiments where the metal complex–DNA mixture was sonicated, may be due to a small contribution from cross-reactions, e.g.

$$Ru(III)-DNA + Ru(I) \rightarrow Ru(II)-DNA + Ru(II)^* \text{ or}$$
$$Ru(II)^*-DNA + Ru(II) \quad (22)$$
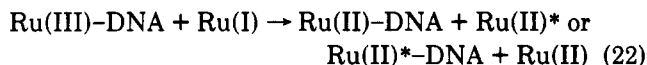
in which degradation of the DNA strand by ultrasound would enhance ECL production by increasing the diffusion coefficient of the bound metal.

The simple equilibrium binding model, used previously for analysis of titration curves from voltammetric experiments involving diffusion of an equilibrium mixture of free and DNA-bound metal complex (*26*, *27*), yields values of K and s in this study that appear to be unreasonably large, compared to those of previous studies. This model assumes that the DNA strand can be saturated with metal complex (i.e., gaps of $<s$ bp are rare or nonexistent). While this model was successful in analyzing binding data in uncomplicated solutions, e.g. 50 mM NaCl (*26*, *27*), in the present case, the presence of surfactants may affect the binding of $Ru(phen)_3^{2+}$. For example, the nonionic surfactant Triton X-100 could associate hydrophobically with the DNA helix, preventing some base pairs from interaction with $Ru(phen)_3^{2+}$. The structurally similar 5-alkylresorcinols (*44*) and a number of other lipophilic species (*45*) bind to DNA via association with the hydrophobic interior of the strand. While the simple model cannot take this into account, direct detection of free and DNA-bound Ru(II) in ECL allows the use of the model of McGhee and von Hippel. The agreement between our results and previous determination of s for the Ru-$(phen)_3^{2+}$–DNA system provides additional evidence for the validity of the assumptions used. Finally we might mention that similar ECL studies with $Ru(bpy)_3^{2+}$ show no binding effect of DNA, consistent with the known lack of intercalative interaction of this species with DNA (*46*). Further related studies with other metal chelates are in progress.

CONCLUSIONS

Electrogenerated chemiluminescence (ECL) can be applied to the study of the binding of certain luminescent metal complexes to DNA. Selection of the proper ECL-generating system, e.g. with an anionic precursor ($C_2O_4^{2-}$) of a strong reductant ($CO_2^{\bullet-}$), allows the independent determination of free and DNA-bound complex. ECL data from titration experiments can be applied directly to the same binding models used in equilibrium dialysis and spectrophotometric determinations, without the need to consider diffusion coefficients (required for voltammetric measurements) or ECL efficiencies. While the range of useful metal chelates that show ECL is small, these should provide useful tags of DNA and are capable of measurements at very low metal chelate concentrations.

ACKNOWLEDGMENT

LITERATURE CITED

(1) Faulkner, L. R., and Bard, A. J. (1977) Techniques of electrogenerated chemiluminescence. In *Electroanalytical Chemistry*, Vol. 10 (A. J. Bard, Ed.) pp 1–95 and references therein, Marcel Dekker, New York.

(2) Tokel, N. E., and Bard, A. J. (1972) Electrogenerated chemiluminescence IX. Electrochemistry and emission from systems containing tris(2,2'-bipyridine)ruthenium(II) and dichloride. *J. Am. Chem. Soc. 94*, 2862.

(3) Tokel-Takvoryan, N. E., Hemingway, R. E., and Bard, A. J. (1973) Electrogenerated chemiluminescence XIII. Electrochemical and electrogenerated chemiluminescence studies of ruthenium chelates. *J. Am. Chem. Soc. 95*, 6582.

(4) Luttmer, J. D., and Bard, A. J. (1981) Electrogenerated chemiluminescence 38. Emission intensity-time transients in the tris(2,2'-bipyridine)ruthenium(II) system. *J. Phys. Chem. 85*, 1155.

(5) Abruña, H. D., and Bard, A. J. (1982) Electrogenerated chemiluminescence. 40. A chemiluminescent polymer based on the tris(4-vinyl-4'-methyl-2,2'-bipyridyl)ruthenium(II) system. *J. Am. Chem. Soc. 104*, 2641.

(6) Gonzales-Velasco, J., Rubinstein, I., Crutchley, R. J., Lever, A. B. P., and Bard, A. J. (1983) Electrogenerated chemiluminescence. 42. Electrochemistry and electrogenerated chemiluminescence of the tris(2,2'-bipyrazine)ruthenium(II) system. *Inorg. Chem. 22*, 822.

(7) Chang, M.-M., Saji, T., and Bard, A. J. (1977) Electrogenerated chemiluminescence. 30. Electrochemical oxidation of oxalate ion in the presence of luminescers in acetonitrile solutions. *J. Am. Chem. Soc. 99*, 5399.

(8) Rubinstein, I., and Bard, A. J. (1981) Electrogenerated chemiluminescence. 37. Aqueous electrogenerated chemiluminescence systems based on $Ru(2,2'$-bipyridine$)_3^{2+}$ and oxalate or organic acids. *J. Am. Chem. Soc. 103*, 512.

(9) White, H. S., and Bard, A. J. (1982) Electrogenerated chemiluminescence. 41. Electrogenerated chemiluminescence and chemiluminescence of $Ru(2,2'$-bipyridine$)_3^{2+}$-peroxydisulfate system in acetonitrile–water solutions. *J. Am. Chem. Soc. 104*, 6891.

(10) Ege, D., Becker, W. G., and Bard, A. J. (1984) Electrogenerated chemiluminescent determination of $Ru(bpy)_3^{2+}$ at low levels. *Anal. Chem. 56*, 2413.

(11) Barton, J. K. (1983) Tris(phenanthroline) metal complexes: probes for DNA helicity. *J. Biomol. Struct. Dyn. 1*, 621.

(12) Barton, J. K. (1985) Simple coordination complexes: drugs and probes for DNA structure. *Comments Inorg. Chem. 3*, 321.

(13) Barton, J. K. (1986) Metals and DNA: molecular left-handed complements. *Science 233*, 727.

(14) Barton, J. K., and Lolis, E. (1985) Chiral discrimination in the covalent binding of Bis(phenanthroline)dichlororuthenium-(II) to B-DNA. *J. Am. Chem. Soc. 107*, 708.

(15) Barton, J. K., Danishefsky, A. T., and Goldberg, J. M. (1984) Tris(phenanthroline)ruthenium(II): stereoselectivity in binding to DNA. *J. Am. Chem. Soc. 106*, 2172.

(16) Barton, J. K., Basile, L. A., Danishefsky, A., and Alexandrescu, A. (1984) Chiral probes for the handedness of DNA helices: enantiomers of tris(4,7-diphenylphenanthroline)-ruthenium(II). *Proc. Natl. Acad. Sci. U.S.A. 81*, 1961.

(17) Kumar, C. V., Barton, J. K., and Turro, N. J. (1985) Photophysics of ruthenium complexes bound to double helical DNA. *J. Am. Chem. Soc. 107*, 5518.

(18) Barton, J. K., Goldberg, J. M., Kumar, C. V., and Turro, N. J. (1986) Binding modes and base specificity of tris-(phenanthroline)ruthenium(II) enantiomers with nucleic acids: tuning the stereoselectivity. *J. Am. Chem. Soc. 108*, 2081.

(19) Goldstein, B. M., Barton, J. K., and Berman, H. M. (1986) Crystal and molecular structure of a chiral-specific DNA-binding agent: tris(4,7-diphenylphenanthroline)ruthenium-(II). *Inorg. Chem. 25*, 842.

(20) Mei, H.-Y., and Barton, J. K. (1986) A chiral probe for A-form helices of DNA and RNA: tris(tetramethylphenanthroline)-ruthenium(II). *J. Am. Chem. Soc. 108*, 7414.

(21) Basile, L. A., and Barton, J. K. (1987) Design of a double-strand DNA cleaving agent with two polyamine metal-binding arms: $Ru(DIP)_2$ macro^{n+}. *J. Am. Chem. Soc. 109*, 7548.

(22) Basile, L. A., Raphael, A. L., and Barton, J. K. (1987) Metal activated hydrolytic cleavage of DNA. *J. Am. Chem. Soc. 109*, 7550.

(23) Adam, W., and Cilento, G. (Eds.) (1982) *Chemical and Biological Generation of Excited States* Academic Press, New York.

(24) Cormier, M. J., Hercules, D. M., and Lee, J. (Eds.) (1973) *Chemiluminescence and Bioluminescence* Wiley, New York.

(25) Schölmerich, J., Andreesen, R., Kapp, A., Ernst, M., and Woods, W. G. (1987) *Bioluminescence and Chemiluminescence* Wiley, Chichester.

(26) Carter, M. T., and Bard, A. J. (1987) Voltammetric studies of the interaction of tris(1,10-phenanthroline)cobalt(II) with DNA. *J. Am. Chem. Soc. 109*, 7528.

(27) Carter, M. T., Rodriguez, M., and Bard, A. J. (1989) Voltammetric studies of the interaction of metal chelates with DNA. 2. Tris-chelated complexes of cobalt(III) and iron(II) with 1,10-phenanthroline and 2,2'-bipyridine. *J. Am. Chem. Soc. 111*, 8901.

(28) Reichmann, M. E., Rice, S. A., Thomas, C. A., and Doty, P. (1954) A further examination of the molecular weight and size of desoxypentose nucleic acid. *J. Am. Chem. Soc. 76*, 3047.

(29) Lin, C.-T., Böttcher, W., Chou, M., Creutz, C., and Sutin, N. (1976) Mechanism of the quenching of the emission of substituted polypyridineruthenium(II) complexes by iron(III), chromium(III), and europium(III) ions. *J. Am. Chem. Soc. 98*, 6536.

(30) Jacobsen, E., and Sawyer, D. T. (1968) Electrochemical oxidation of oxalate ion in dimethylsulfoxide at a gold electrode. *J. Electroanal. Chem. 16*, 361.

(31) Anson, F. C., and Schultz, F. A. (1963) Effect of adsorption and electrode oxidation on the oxidation of oxalic acid at platinum electrodes. *Anal. Chem. 35*, 1114.

(32) Leland, J. K. IGEN, Inc., private communication.

(33) Noffsinger, J. B., and Danielson, N. D. (1987) Generation of chemiluminescence upon reaction of aliphatic amines with tris(2,2'-bipyridine)ruthenium(III). *Anal. Chem. 59*, 865.

(34) Scatchard, G. (1949) The attractions of proteins for small molecules and ions. *Ann. N. Y. Acad. Sci. 51*, 660.

(35) McGhee, J. D., and von Hippel, P. H. (1974) Theoretical aspects of DNA-protein interactions: co-operative and non-co-operative binding of large ligands to a one-dimensional homogeneous lattice. *J. Mol. Biol. 86*, 469.

(36) Kaifer, A. E., and Bard, A. J. (1985) Micellar effects on the reductive electrochemistry of methyl viologen. *J. Phys. Chem. 89*, 4876.

(37) Ouyang, J., and Bard, A. J. (1988) Electrogenerated chemiluminescence 50. Electrochemistry and electrogenerated chemiluminescence of micelle solubilized $Os(bpy)_3^{2+}$. *Bull. Chem. Soc. Jpn. 61*, 17.

(38) Smith, P. J., and Mann, C. K. (1969) Electrochemical dealkylation of aliphatic amines. *J. Org. Chem. 34*, 1821.

(39) Manning, G. (1978) The molecular theory of polyelectrolyte solutions with applications to the electrostatic properties of polynucleotides. *Q. Rev. Biophys. 11*, 179.

(40) Berg, O. G., and von Hippel, P. H. (1985) Diffusion controlled macromolecular interactions. *Ann. Rev. Biophys. Chem. 14*, 131.

(41) Kelly, J. M., Tossi, A. B., McConnell, D. J., and OhUigin, C. (1985) A study of the interactions of some polypyridylruthenium(II) complexes with DNA using fluorescence spectroscopy, topoisomerisation and thermal denaturation. *Nucleic Acids Res. 13*, 6017.

(42) Fromhertz, P., and Rieger, B. (1986) Photoinduced electron transfer in DNA matrix from intercalated ethidium to condensed methyl viologen. *J. Am. Chem. Soc. 108*, 5361.

(43) Atherton, S. J., and Beaumont, P. C. (1987) Laser flash photolysis of DNA-intercalated ethidium bromide in the presence of methyl viologen. *J. Phys. Chem. 91*, 3993.

(44) Scannell, R. T., Barr, J. R., Murty, V. S., Reddy, K. S., and Hecht, S. M. (1988) DNA strand scission by naturally occurring 5-alkylresorcinols. *J. Am. Chem. Soc. 110*, 3650.

(45) Baguley, B. C. (1982) Nonintercalative DNA-binding antitumor compounds. *Mol. Cell. Biochem. 43*, 167.

(46) Schmidt, N., and Bard, A. J., unpublished results.

Registry No. $Ru(phen)_3^{2+}$, 22873-66-1.